Food Innovation and Advances

ARTICLE

Open Access

https://doi.org/10.48130/fia-0024-0032

*Food Innovation and Advances* **2024**, 3(4): 332–343

# pH/glucose dual-responsive protein-based hydrogels with enhanced adhesive and antibacterial properties for diabetic wound healing

Shuhua Yin[1#], Maoping Duan[1#], Matthias Fellner[2], Zhongjiang Wang[3], Chenyan Lv[1,4], Jiachen Zang[1], Guanghua Zhao[1,4] and Tuo Zhang[1,4*]

[1] *Center of Food Colloids and Delivery for Function, College of Food Science and Nutritional Engineering, China Agricultural University, Beijing 100083, China*
[2] *Biochemistry Department, School of Biomedical Sciences, University of Otago, Dunedin 9054, New Zealand*
[3] *College of Food Science, Northeast Agricultural University, Harbin 150030, Heilongjiang, China*
[4] *Beijing Key Laboratory of Functional Food from Plant Resources, College of Food Science and Nutritional Engineering, China Agricultural University, Beijing 100083, China*
[#] Authors contributed equally: Shuhua Yin, Maoping Duan
* Corresponding author, E-mail: zhangtuo@cau.edu.cn

## Abstract

Designing a wound dressing that offers excellent antibacterial properties while providing dual pH/glucose responsiveness for diabetic wound healing remains a considerable challenge. Herein, a 3D cross-linked native protein hydrogel was constructed through a Schiff base reaction based on -$NH_2$ in paramyosin (PM) and -CHO in oxidized dextran (ODA) under mild conditions. Within the hydrogel, both amikacin and glucose oxidase were encapsulated during gelation. The resulting hydrogel exhibited favorable rheological properties, featuring self-healing, antibacterial activity, tissue adhesiveness, and excellent biocompatibility. Notably, the hydrogel demonstrated excellent pH/glucose dual-responsive properties. In infected wounds, the Schiff base bonds dissociated due to low pH, while in uninfected wounds with high blood glucose levels, the encapsulated glucose oxidase was functional, which also lowered the local pH level and dissociated the Schiff base bonds. Furthermore, the hydrogel quickly achieved pH/glucose dual responsiveness, leading to increased amikacin release to reduce bacterial invasion, alleviate oxidative stress, promote re-epithelialization and collagen deposition, and eventually accelerate diabetic wound healing. Collectively, the constructed hydrogel offers brand-new viewpoints on glucose-responsive biomaterials for diabetic wound therapy.

**Citation:** Yin S, Duan M, Fellner M, Wang Z, Lv C, et al. 2024. pH/glucose dual-responsive protein-based hydrogels with enhanced adhesive and antibacterial properties for diabetic wound healing. *Food Innovation and Advances* 3(4): 332–343 https://doi.org/10.48130/fia-0024-0032

## Introduction

Diabetes mellitus, a long-term metabolic disorder, presents a major global health and economic challenge. A huge percentage of patients experience diabetic ulcers in the advanced stages of the illness[1]. These wounds are particularly difficult to treat due to long-term inflammation[2], persistent vascular damage[3], and uncontrolled bacterial invasion[4]. Research studies indicated that as much as 25% of diabetics have a higher risk of developing persistent non-healing injuries throughout their lives[5]. The microenvironment of diabetic wounds is notably harsh, featuring high blood glucose levels and compromised immunity, which creates favorable conditions for bacterial growth[6,7]. This, in turn, leads to a decrease in local pH[8], persistent inflammation, and a rise in excessive reactive oxygen types (ROS)[9,10]. The high levels of ROS triggers an inflammatory response that hinders wound tissue regeneration by destroying cells and maintaining the macrophages in the M1 phenotype[11,12]. Therefore, it is important to develop a material that can effectively clear microbial emigration and regulate the microenvironment of the injury site to help with diabetic wound healing.

Current therapeutic strategies aiming at diabetic wounds treatment mainly include oxygen release[13], photothermal therapy[14], honey therapy[15], wound dressing, and engineered protein therapies[16]. Among them, hydrogel dressings with an extracellular matrix-like three-dimensional structures have great advantages and are widely used in diabetic wound treatment[17,18]. Hydrogel can not only increase the speed of wound recovery by absorbing metabolites and supplying a moist atmosphere, but also serve as a reliable medicine delivery vehicle for dealing with diabetic wounds. Many efforts have been made to develop multifunctional and environmental-stimulus-responsive hydrogels for diabetic wound healing. One efficient way to achieve a sensor-responsive process is to introduce reversible covalent chemical bonds into hydrogels. Several types of covalent bonding, including Schiff base, phenylboronate ester bonds, disulfide bonds, metal coordination, and acylhydrazone bonds, have been extensively utilized to develop smart hydrogels that can respond to stimulation by pH, glucose, or hydrogen peroxide[19–21], thus achieving controlled drug release. These dynamic reversible covalent bonds additionally endow the hydrogel with self-healing and injectable characteristics.

Dextran, a polysaccharide produced by bacteria, is extensively used in biomedical applications for its biocompatibility, high natural abundance, cost-effectiveness, and ease of modification[22]. In addition, an oxidized dextran derivative with aldehyde functional groups is an ideal building block or crosslinker to construct hydrogels through the Schiff base reaction, and

the constructed hydrogels often show benign tissue adhesion[23]. Most importantly, the lactic acid and acetic acid produced by bacteria in infected wounds result in an acidic physiological environment (4.5–6.5) locally[24,25]. In the existence of $O_2$, glucose oxidase could convert glucose into gluconic acid and $H_2O_2$, which possess both hypoglycemic and antibacterial activity[26,27]. Additionally, the production of gluconic acid creates an acidic environment, which can cause the fragmentation of the imine-bond hydrogel[28], offering the potential for controlled drug release in biomedical applications.

Hydrogels originating from all-natural polymers have actually drawn focus owing to their outstanding biocompatibility and diverse biological function[29]. Protein-based hydrogels not only maintain the properties of polymer-based materials, but also possess specific controllable structural functionalities and inherent biodegradability[30]. The benefits of these characteristics and their potential applications ranging from drug delivery, tissue engineering, and re-generative medicine have been well studied[31]. A Schiff base is commonly developed *via* the reaction in between compounds containing aldehyde (or ketone) teams and amino groups, resulting in the formation of imine groups (-C=N-). Compared to other covalent linkers, Schiff base structures exhibit remarkable reversibility in response to pH changes, as the pH drops, these bonds become less stable[32]. Denatured proteins and amino-modified compounds serve as common building blocks for constructing hydrogels through the formation of Schiff bases[33–35]. However, natural protein-based hydrogels constructed by taking advantage of glucose sensitivity from glucose oxidase and pH sensitivity from a Schiff base linkage for diabetic wound healing remains unexplored.

In this research, a naturally derived cross-linked smart protein hydrogel was developed based on dynamic Schiff base bonds between $-NH_2$ in paramyosin (PM), a natural fibrous protein reported in our previous study[36], and -CHO in oxidized dextran (ODA) to realize local controlled release in the therapy of diabetic wounds (Fig. 1). Through the effective encapsulation of glucose oxidase and amikacin, the hydrogel was endowed with glucose stimulation responsiveness and antibacterial activity, respectively. The physicochemical properties of the hydrogel were explored, including its rheological properties, self-healing and injectable behavior, adhesion behavior, and amikacin stimuli-responsive release under different pH/glucose conditions. On top of that, the anti-bacterial activity, *in vitro* blood biocompatibility, and cytotoxicity of the hydrogel were also evaluated. Finally, the diabetic wound model established in mice was developed and the effect of the hydrogel on promoting wound healing through epithelial regeneration and collagen deposition was determined. Overall, the findings indicate that the hydrogels constructed are potentially effective wound dressings for accelerating the healing of diabetic injuries.

## Materials and methods

### Materials

Dextran (Mw 70 kDa), glucose oxidase (from Aspergillus), amikacin, and sodium periodate was purchased from Aladdin (Shanghai, China). Dialysis membranes (molecular cutoff 3500 Da), hydroxylamine hydrochloride, and cell counting kit8 (CCK8) were obtained from Solarbio (Beijing, China). Fetal bovine serum (FBS), DMEM, and TGF-$\beta$1, $\alpha$-SMA, TNF-$\alpha$, and GAPDH antibodies were purchased from Sigma-Aldrich (St. Louis, USA). Chitosan medical hydrogel was bought from Humanwell Medical care Co., Ltd. (Wuhan, China) and used as a positive control for the treatment of diabetic injury recovery.

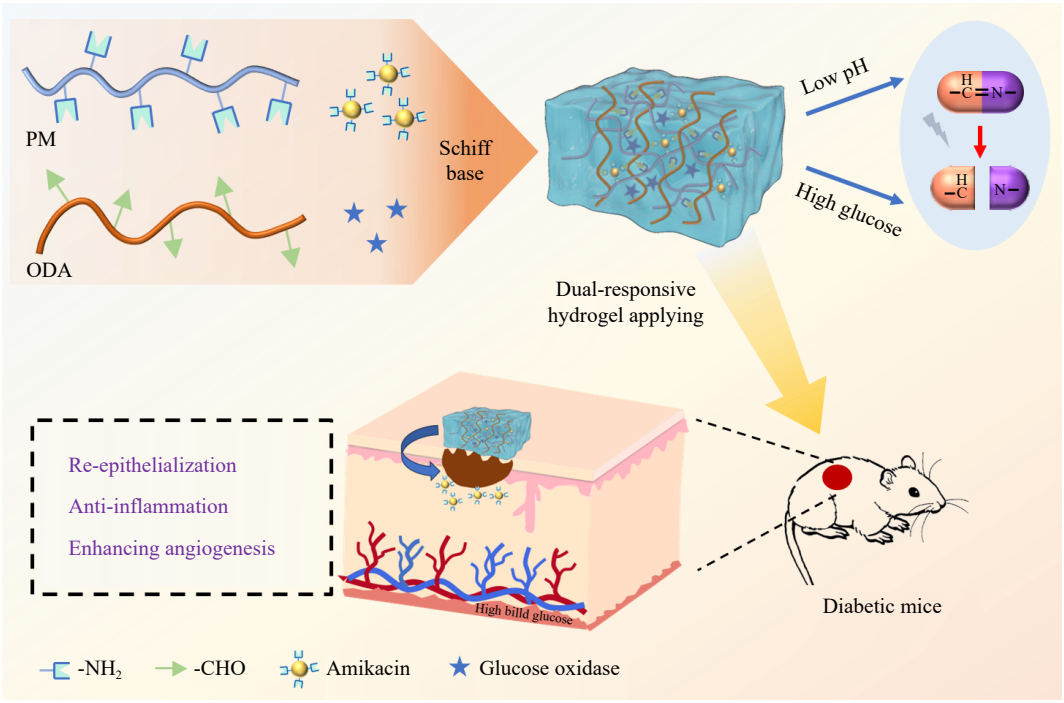


**Fig. 1** Schematic illustration of the preparation procedures of the pH/glucose dual-responsive hydrogel dressing for promoting chronic wound healing in the diabetic C57BL/6N mouse model.

## Synthesis and characterization of the oxidized dextran

The production process for oxidized dextran (ODA) followed a previously published study[37]. Rapidly, dextran and salt periodate were mixed with deionized water and stirred at room temperature. Subsequently, ethylene glycol was introduced to terminate the reaction. The ODA solution was subjected to thorough dialysis against deionized water, followed by lyophilization to obtain ODA powder. The structure of the produced ODA powder was analyzed using Fourier-transform infrared spectroscopy (FTIR) and UV-vis. The oxidation state of the oxidized dextran was determined by hydroxylamine hydrochloride titration[38].

## Preparation and characterization of hydrogels

The extraction and purification procedure of paramyosin (PM) from oysters (*Crassostrea gigas*) followed our previous publication[36]. Briefly, the adductor muscular tissue was diced and homogenized with phosphate buffer (150 mM $NaH_2PO_4$ and $Na_2HPO_4$, 100 mM KCl, pH 6.5). The homogenized solution was then centrifuged and the precipitate was washed with 50 mM $NaHCO_3$, followed by another round of centrifugation. The remaining precipitate was dissolved in deionized water with stirring for 30 min. After centrifugation, the supernatant was precipitated with 35% ammonium sulfate. The fully dialyzed sample was loaded to an ion exchange column and the purified protein was assessed by SDS-PAGE. Subsequently, the purified protein was concentrated to 10 mg·mL$^{-1}$, and the lyophilized oxidized dextran was completely dissolved at a 50 mg/mL concentration in deionized water. The PM and ODA solutions were mixed uniformly in equal volumes, and glucose oxidase and amikacin were added to the mixed solution to obtain different hydrogels within 30 min. The hydrogels encapsulating only glucose oxidase, only amikacin, and binary components (glucose oxidase and amikacin) were named POG, POK, and POGK, respectively. The final concentrations of glucose oxidase and amikacin in the hydrogel were 30.5 μM and 20 mM, respectively. FTIR spectra of the hydrogels was measured on a Nicolet 670 FTIR (Thermo Fisher Scientific, Inc, USA) spectrometer using the attenuated total reflectance model with the wavenumber range over 400–4,000 cm$^{-1}$. The morphological structure of these hydrogels was determined using a cryo-scanning electron microscope. The protein hydrogel was placed in the circular hole of the copper sample stage and frozen using the liquid nitrogen slurry method. Then, the sample was sublimated at −75 °C for 30 min to prevent the surface from being covered with ice. Finally, after conductive spraying, the sample was observed with a HITACHI S-4800 microscope.

## Rheology analysis

The rheological properties of hydrogels were assessed using a rotational rheometer (TA Instruments, USA). During the strain sweep, the hydrogel was applied onto a parallel plate, and the strain sweep was conducted to evaluate the linear viscoelastic properties of the hydrogels. Frequency sweeps of the hydrogels were executed over a variety of 0.01−100 Hz at 1% stress. To evaluate the self-healing properties of the hydrogel, a step strain sweep was performed, alternating between low stress (1%, 60 s for each period) to high stress (200%, 60 s for every interval) for five cycles. The injectability of the hydrogels was identified making use of a flow test mode with shear rate ranging from 0.01 to 100 s$^{-1}$.

## Characterization of injectability and adhesive performance

To evaluate the injectable residential or commercial properties of the hydrogel, the POGK hydrogel was filled into a syringe and after that injected into various letters. The injection processes were photographed to document the behavior of the hydrogel. The adhesive capability of the hydrogel was assessed by positioning the POGK hydrogel, formed into a cylindrical shape, on materials with different properties. The samples were then inverted to observe whether the gel adhered to the materials or fell off.

## Swelling capacity analysis

The swelling ratio of the POG and POGK hydrogels was measured gravimetrically. Briefly, pre-weighed lyophilized hydrogels were dipped in PBS solution (pH 7.4) for approximately 8 h. At particular time intervals, the swollen hydrogels were taken out from the PBS remedy, and free liquid on the surface was gently removed. Then, the weight of the swollen hydrogels was taken and recorded as Wt. The swelling ratio was calculated utilizing the list below equation: Swelling ratio (%) = $(W_t - W_0) / W_0 \times 100\%$, where, $W_t$ and $W_0$ represent swollen and lyophilized hydrogels, respectively.

## Drug release analysis

Here, the POGK hydrogel was immersed in PBS solution (pH 7.4 or 5.5), with or without the visibility of sugar (25 mM), at a consistent temperature level of 37 °C. At specific time intervals, a certain volume of release solution was removed and an equal volume of fresh solution was added. The concentration of amikacin released was determined using the o-phthalaldehyde method[39]. Briefly, o-phthalaldehyde was dissolved in borate buffer (200 mM, pH 10.5) with the addition of mercaptoethanol. The pH was adjusted to 10.5 with a final fixed volume of 100 mL to obtain the o-phthalaldehyde test solution (PHT). Subsequently, 300 μL PHT and 900 μL isopropanol were added to 300 μL of the hydrogel release solution and heated at 60 °C for 15 min. After cooling, the $OD_{333}$ value of the sample was measured using a UV-vis spectrophotometer (Varian, USA).

## Antibacterial assay

To evaluate the anti-bacterial efficiency of the hydrogels, *E. coli* and *S. aureus* were used in this experiment. First, hydrogel precursor was added to the center well of a 96-well plate. After hydrogels formation, bacterial suspension ($10^4$ CFU) was added to the well, and afterwards cultured at 37 °C for 4 h. Subsequently, PBS was used to resuspend the microorganisms, and the bacterial suspension was inoculated on an LB agar plate for bacterial enumeration. The kill rate was computed by making use of the formula: Kill rate (%) = (Bacterial count of control survivors − Bacterial count of hydrogel groups) / Bacterial count of control survivors × 100%.

## Hemolysis test

Mouse blood was centrifuged to separate red blood cells (RBCs), which were then suspended at a concentration of 2% in PBS solution (pH 7.4). Next, to act as positive and negative controls, the RBC solution was diluted with Triton X-100 and PBS, respectively. The hydrogel samples were mixed with RBC suspension and incubated at 37 °C. Following incubation, the RBC solution was centrifuged, and the $OD_{540}$ value of the supernatant sample was recorded. The hemolytic ratio (%) was evaluated as $(A_{sample} - A_{negative}) / (A_{positive} - A_{negative}) \times 100\%$.

### Cellular biocompatibility assay

The Cell Counting Kit (CCK-8) reagent was used to evaluate the cytocompatibility of the hydrogels. HUVECs and NIH 3T3 cells were cultured in a complete DMEM medium at 37 °C in a 5% $CO_2$ environment after being seeded in a 96-well plate. After incubation, hydrogel samples were added to the medium in the cell well. Subsequently, CCK-8 solution was used to incubated with cells for another 2 h. The $OD_{450}$ value was then determined using a microplate reader (model 680, Bio-Rad, USA).

### *In vivo* wound healing assessment

The C57BL/6N mice were purchased from Beijing Vital River Laboratory Animal Innovation Co., Ltd (Beijing, China). The animal studies followed the guidelines set by the National Research Council's Overview for the Care and Use of Laboratory Animals and were approved by the Animal Experimental Ethical Inspection Board of China Agricultural College (Aw31213202-4-1). Male C57BL/6N mice, aged six weeks, were administered intraperitoneally with streptozotocin (50 mg·kg$^{-1}$) for four consecutive days until their fasting blood glucose level exceeded 16.7 mmol·L$^{-1}$. The diabetic mice were divided into four groups (n = 8): control, POG hydrogel, POGK hydrogel, and positive control. Subsequently, the mice were rendered unconscious with sodium pentobarbital and a full-thickness 8 mm diameter wound was created. Various hydrogel examples were put on the injury sites and freshened every two days throughout the experimental period. On the other hand, injury locations were photographed and measured using Image J software program on days 0, 3, 7, 10, and 14. The wound closure rate (%) was determined using the following formula: Injury closure (%) = $(A_0 - A_t) / A_0 \times 100\%$, where, $A_0$ and $A_t$ represent the initial wound location and the wound location at various time points, respectively.

### Histological analysis

On day 14, the mice were euthanized and samples of skin were gathered from the areas surrounding the diabetic wound sites. Formaldehyde solution (4%, W/V) was used to fix the tissue samples. Then, the fixed tissues were embedded and stained with H&E and Masson's trichrome complying with standard operating procedures. Collagen deposition of the wound tissues was determined using ImageJ software.

### Western blot assay

Wound tissues were lysed on ice with RIPA buffer, and then the lysates were centrifuged to obtain the sample supernatants. The protein separations were performed using a 12% SDS-PAGE gel. Following the transfer of proteins to the polyvinylidene fluoride membrane, the membrane was blocked with skim milk for a duration of 2 h. Subsequently, the membrane was treated with primary antibodies targeting TGF-$\beta$, $\alpha$-SMA, TNF-$\alpha$, and GAPDH overnight at a temperature of 4 °C. Following the TBST wash, the membrane layers were incubated with secondary antibodies for 2 h at room temperature. After thoroughly washing with TBST, the protein bands were detected using an enhanced chemiluminescent reagent through Tanon 4800 image. The protein expression levels were determined using the ImageJ software.

### Statistical analysis

Every single data point was collected from a minimum of three iterations and represented as the mean ± standard deviation. Statistical significance was determined using one-way analysis of variance (ANOVA), and $p < 0.05$ was considered statistically significant.

## Results and discussion

### Construction and characterization of hydrogels

Paramyosin (PM) was purified from oyster adductor muscle cells using the treatment outlined in Supplementary Fig. S1a. SDS-PAGE analysis revealed a solitary band corresponding to a molecular weight of 99 kDa (Fig. 2a). In addition, the 3D structure of PM was predicted by TR-Rosetta online website based on its amino acid sequence[36]. There are approximately 149 free amino groups present on lysine and arginine residues, which are evenly distributed on the fibrous protein surface, making it a suitable candidate for Schiff base reaction with aldehyde polymer (Supplementary Fig. S1b). To obtain an oxidized dextran (ODA) polymer with aldehyde groups, dextran was oxidized using sodium periodate. The chemical structure of ODA was characterized using UV-vis spectrum and FTIR analysis. The UV-vis spectrum of ODA revealed an absorption peak at 237 nm compared to dextran, indicating the visibility of aldehyde groups due to dextran oxidation (Supplementary Fig. S2)[40]. Furthermore, FTIR spectroscopy confirmed the successful preparation of the ODA polymer, as evidenced by the new peak presented at 1,734 cm$^{-1}$, corresponding to the stretching vibration of the aldehyde group (Fig. 2b)[41]. The oxidation degree of ODA was determined to be 44.55% using hydroxylamine hydrochloride titration (Supplementary Fig. S3). Taken together, these results demonstrated that the ODA was successfully synthesized and could be utilized for hydrogel construction.

Subsequently, equal volumes of PM and ODA solutions were combined to fabricate hydrogels through a Schiff base reaction. Glucose oxidase and amikacin, an aminoglycoside antibiotic, were incorporated into the hydrogel, imparting it with glucose-responsive and antibacterial properties. The hydrogel formed after 30 min of incubation. Figure 2c provides a representative example, showing the appearance before and after gelation. FTIR spectra was used to examine the chemical structure of hydrogels encapsulating only glucose oxidase (POG hydrogel) and both components (POGK hydrogel). As shown in Fig. 2b, compared with the ODA, the stretching vibration of the aldehyde group at 1,734 cm$^{-1}$ disappeared, and the new peak at 1,652 cm$^{-1}$ in both hydrogel spectra was assigned to the stretching vibration of the imine structure (-C=N-)[42], indicating the formation of Schiff base bonds. Scanning electron microscopy (SEM) was used to observe the microstructure of the hydrogels, revealing that both hydrogels possess uniform 3D porous network structures (Fig. 2c). In the context of wound dressing, the porous structure is crucial to facilitate cell migration, nutrient exchange, and tissue regeneration[40]. Moreover, the swelling ratio of the POG and POGK hydrogels was evaluated gravimetrically. Both hydrogels showed good swelling ability, with maximum swelling ratios being reached after 6 h at 672.25% ± 28.52% for the POG hydrogel and 721.89% ± 23.01% for the POGK hydrogel (Supplementary Fig. S4). These results demonstrate that the constructed hydrogels have a superb capacity to absorb wound exudate.

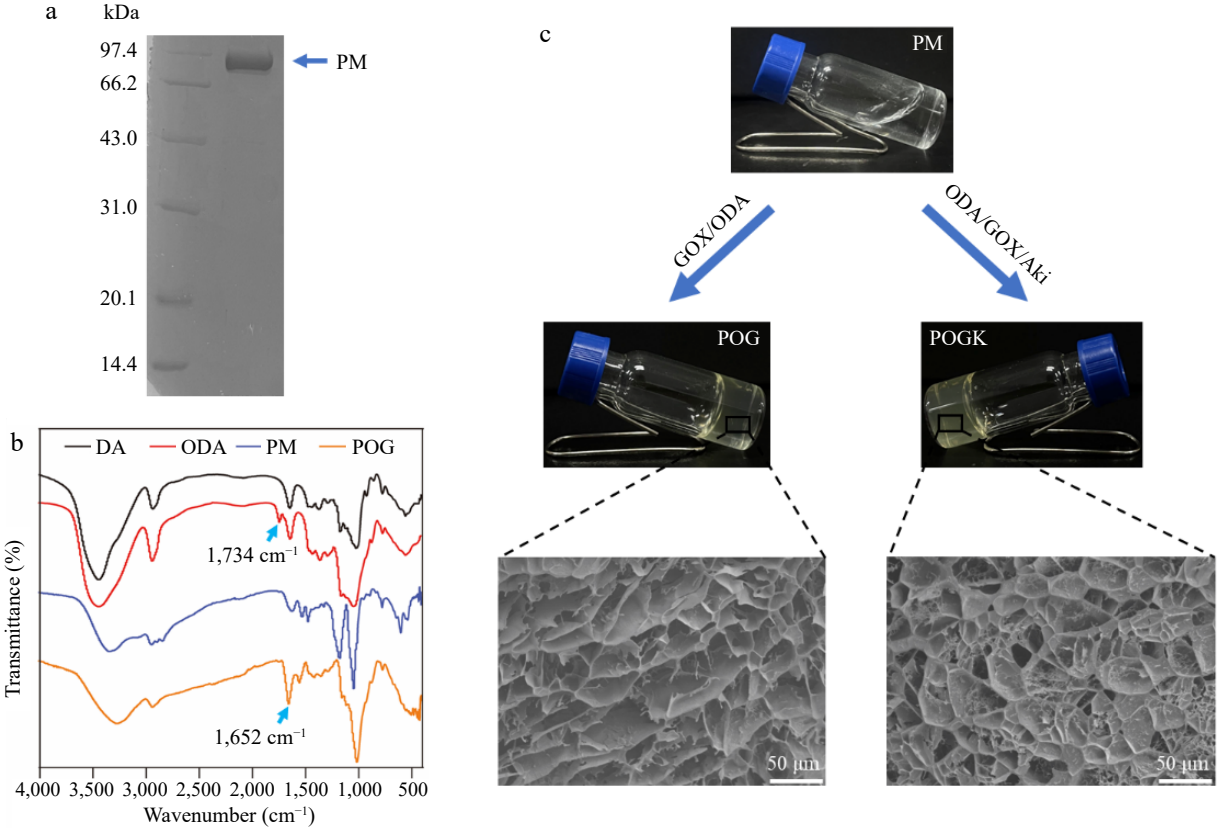


**Fig. 2** Characterization of the hydrogels. (a) SDS-PAGE analysis of the purified paramyosin. (b) FTIR spectra of the DA, ODA, POG, and POGK. (c) Optical photos of the formation of POG and POGK hydrogels. The inset images were the SEM observations of POG and POGK hydrogels.

## Rheological properties and injectable and adhesive behavior of hydrogels

Rheological experiments were conducted to investigate the mechanical properties of the hydrogels under varying strain and frequency. As shown in Fig. 3a, a strain amplitude sweep was executed to identify the critical strain point for maintaining the hydrogel morphology. The critical strain value of POG and POGK hydrogels was found to be 193.1% and 217.3%, respectively. Taking the POGK hydrogel as an example, when the strain exceeded 217.3%, the loss modulus (G″) exceeded the storage modulus (G′), indicating that the hydrogel was disrupted and transitioned to a quasi-liquid state. The appropriate critical strain value ensures that the hydrogel will flow smoothly when an external force is applied, making it easy to inject into the wound site through a syringe or catheter. Additionally, the frequency sweep demonstrated that both hydrogels exhibited frequency-independent behavior and maintained the hydrogel elastic network as the frequency changed (Fig. 3b). Based on dynamic covalent bonding, the mechanical properties of the hydrogel effectively match the elastic modulus of biological tissues (0.5–500 kPa)[43], suggesting that it could be a prospective candidate for a wearable dressing to accelerate wound healing. In addition, a step strain measurement at a fixed frequency of 1 Hz was used to describe the self-healing properties of hydrogels. As shown in Fig. 3c and d, under a high strain of 300%, the hydrogels were destroyed and changed into a liquid state characterized by G″ greater than G′. On the other hand, when the strain was changed to 1%, the G′ and G″ quickly recovered to their original values and reconstructed the intact gel network, demonstrating the exceptional self-healing properties of the hydrogels. An optimal diabetic wound dressing should have favorable injectability to fill irregularly shaped wounds well, decrease bacterial infection, and accelerate injury closure. The injectability of the hydrogels was assessed through viscosity measurements. Both the POG and POGK hydrogels had high viscosity at low shear rates. However, as the shear rate boosted, the viscosity of both hydrogels decreased (Supplementary Fig. S5). This behavior indicates that both POG and POGK have good shear-thinning ability and are easily injectable. In addition, as shown in Fig. 3e, the hydrogels could be easily and constantly squeezed out from the pinhole syringe without obstructing or breaking. Moreover, the hydrogel could be used to write letters using the syringe, indicating the superior injectable behavior of the hydrogel. These self-healing and injectable properties were attributed to the dynamic Schiff base bonds between the two-component polymer[44]. Self-adhesion is another exceptional property of the hydrogel. The free amino and carboxyl groups as well as hydroxyl groups in the hydrogel system undergo non-covalent interactions with the substrate surfaces, thus endowing the beneficial bio-adhesive properties[45]. As depicted in Fig. 3f, the hydrogel firmly adheres to a variety of surfaces, including skin, rubber, glass, plastic, and steel.

## pH/glucose dual-responsive release behavior of hydrogels

Glucose oxidase was embedded in the hydrogel through encapsulation and dynamic Schiff base bonds with ODA to perform multiple functions (Fig. 1). Acting as a glucose

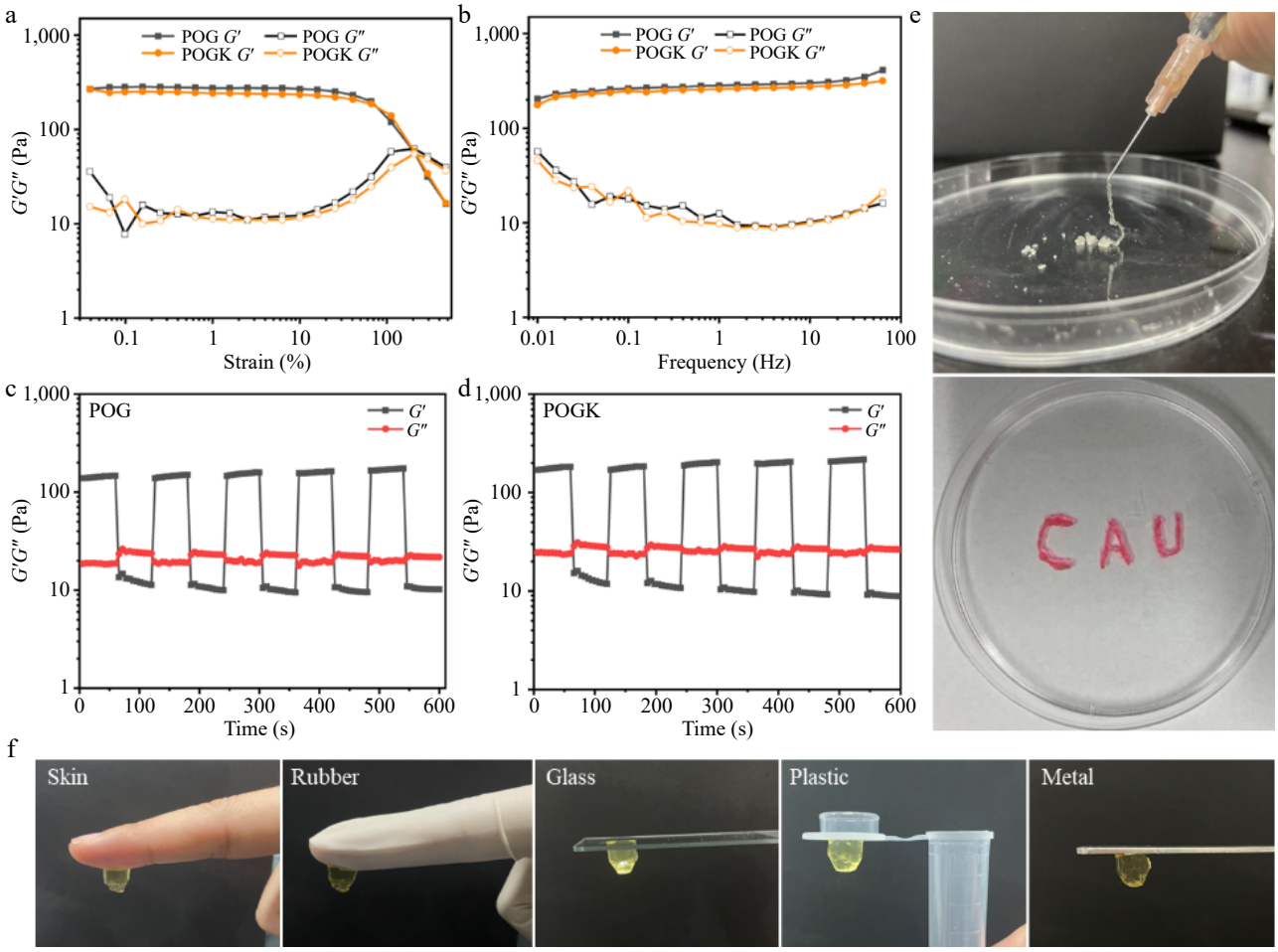


**Fig. 3** Characterization of the rheological properties, injection ability, and adhesion behavior of the protein hydrogels. (a) Strain sweep measurement of POG and POGK hydrogels with a set frequency of 1 Hz. (b) Dynamic frequency–sweep measurements of the POG and POGK hydrogels. Step-strain measurements of the (c) POG, and (d) POGK over five cycles at different strain. (e) Photos showing the injection of the POGK hydrogel. The red color of the hydrogel was from the embedded Rhodamine 6G. (f) Photographs of POGK hydrogel adhering to skin, rubber, glass, plastic, and steel.

scavenger, glucose oxidase can effectively alleviate hyperglycemic environmental stress and inhibit bacterial growth[46]. Additionally, the catalytically generated gluconic acid could create an acidic environment to facilitate the degradation of the designed Schiff base bonds, thereby achieving the pH and glucose dual responsiveness of the hydrogels. In this study, the pH/glucose dual stimuli-responsive drug release properties of the hydrogels were explored under various conditions. The pH-responsive release of amikacin was examined by exposing the POGK hydrogel to different pH environments. As depicted in Fig. 4a, after 12 h of incubation, the cumulative amikacin release from the POGK hydrogel under pH 5.5 and pH 7.4 conditions was approximately 45.6% and 15.3%, respectively. Notably, the release rate of amikacin from the hydrogels was significantly higher in the acidic environment compared to the physiological environment. This was attributed to the hydrolysis and disruption of the Schiff base structure under acidic conditions[47], leading to the collapse of the hydrogel, thereby allowing for a rapid amikacin release. Given the prolonged inflammatory phase commonly observed in diabetic wounds, which results in an acidic microenvironment[48], the pH-responsive hydrogel, with its enhanced drug-release properties at low pH, holds promise for applications in diabetic wound healing. Furthermore, the glucose-responsive amikacin release in 25 mM glucose was investigated in PBS (pH 7.4), with PBS without glucose used as a control. As shown in Fig. 4b, the amount of sustained drug release from the POGK hydrogel and the accumulation of amikacin in the glucose environment were approximately three times those of the control group. After 12 h, around 40.9% of the amikacin had been released into the glucose-rich environment. It is worth noting that the hydrogel without glucose oxidase (POK hydrogel) exhibited a release behavior similar to that in the PBS buffer, underscoring the pivotal role of the enzyme in achieving the glucose stimulus responsiveness of the POGK hydrogel. Recent evidence has indicated that the engineered bacteria incorporated into the multifunctional hydrogels can secrete lactic acid to maintain an acidic environment in the wound, promote the switch of pro-inflammatory M1 macrophages to anti-inflammatory M2-like macrophages, and accelerate injury recovery[16]. Additionally, the glucuronic acid produced by glucose oxidation not only couples with Schiff base to achieve the glucose responsiveness of the gel, but also has a pKa value of 3.86, similar to that of lactic acid, which could also create an acidic environment and

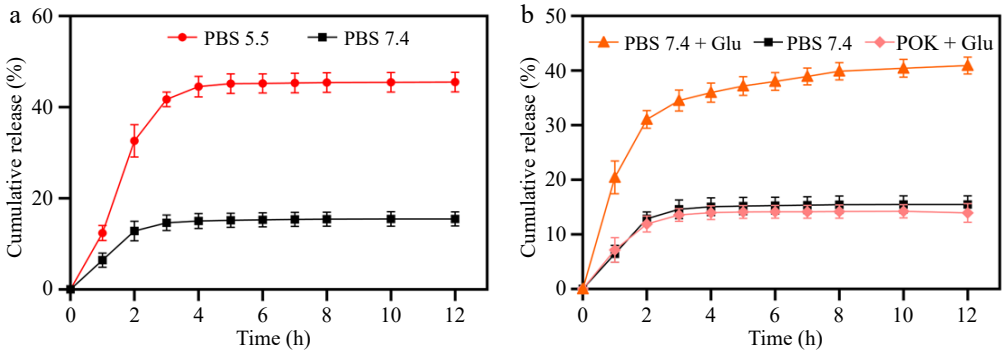


**Fig. 4** Responsive release kinetics of amikacin from POGK hydrogels to (a) pH, and (b) glucose stimulation.

shift macrophages toward an anti-inflammatory phenotype. Most previous studies used boronic ester bonds to construct hydrogels to obtain glucose responsiveness, which required the introduction of some polymeric compounds, but the potential non-biodegradability and cytotoxicity may limit their further application[49–51]. However, in this study, Schiff bases were coupled with enzyme-catalyzed reactions, and dual-responsive protein hydrogels can be easily and rapidly constructed based on natural compounds. Furthermore, another major advantage of PM gels is their one-step gelation character under benign conditions, which is more convenient to encapsulate unstable molecules. Collectively, the synthesized POGK hydrogel possessed unique pH/glucose dual stimuli-responsive drug release characteristics, positioning it as a prospective candidate for diabetic wound healing.

## Antibacterial ability and biocompatibility of the hydrogels

In diabetic wounds, the high-glucose microenvironment increases susceptibility to infection[52]. Therefore, an ideal hydrogel wound dressing should not only have great tissue adhesion and mechanical properties to prevent secondary damage from external factors, but also antibacterial properties to combat invading bacteria, regulate inflammation, and expedite the healing process[53]. In this study, the antibacterial

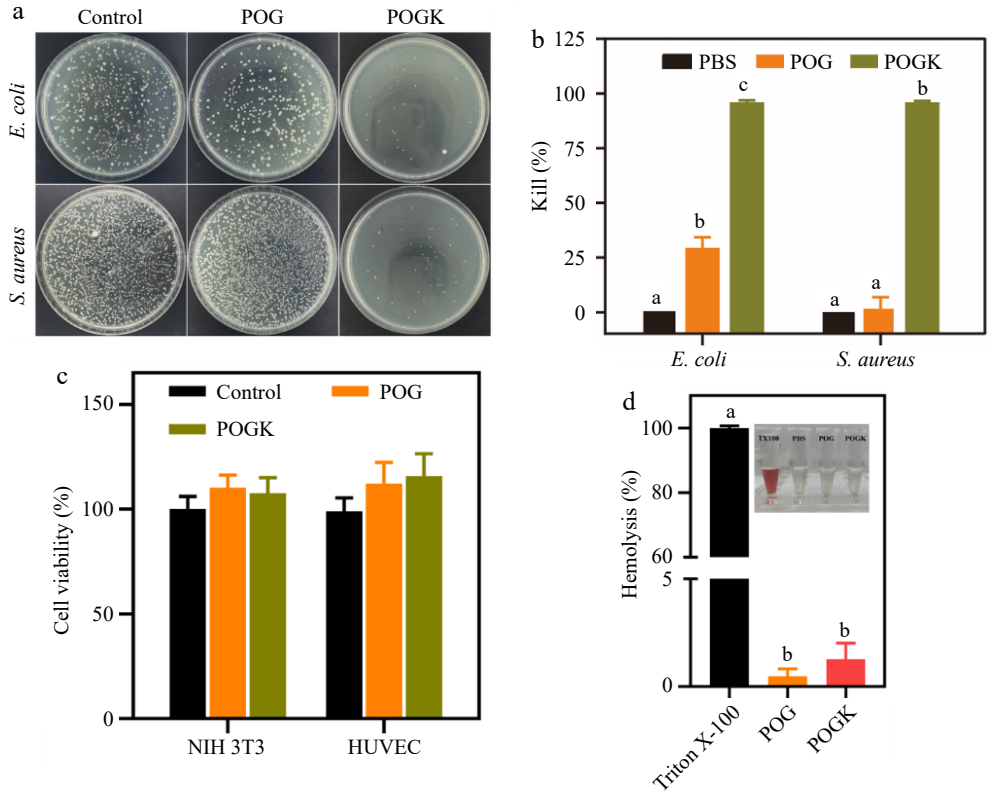


**Fig. 5** *In vitro* bacterial growth inhibition and cytocompatibility of hydrogels. (a) Photos of making it through bacterial clones on LB plates after various treatments. (b) Corresponding bacteria-killing effectiveness against *E. coli* and *S. aureus* (n = 3). (c) Cell feasibility of NIH 3T3 and HUVECs after hydrogel treatment for 6 h. (d) Quantitative hemolysis ratio of 0.1% Triton X-100, POG and POGK hydrogels (n = 3). The insert shows the supernatants of RBCs with different treatments. Different letters in the histograms represent significant differences, $p < 0.05$.

efficiency of the hydrogels was evaluated against the Gram-negative bacterium *E. coli* and Gram-positive bacterium *S. aureus* through the plate-counting method. As depicted in Fig. 5a and b, compared to the PBS group, the hydrogel encapsulating glucose oxidase and amikacin (POGK hydrogel) exhibited notably higher antibacterial activity, with a kill rate against *E. coli* and *S. aureus* of up to 96.1% and 95.5%, respectively. The potent antibacterial effect was attributed to the release of amikacin, which hinders bacterial protein synthesis and disrupts bacterial membrane integrity, ultimately resulting in bacterial demise[54]. Conversely, the relatively weaker bacteriostatic effect of the POG hydrogel may be due to the aldehyde groups in oxidized dextran, which can interact with the amino group of functional proteins on the bacterial surface, causing protein coagulation and precipitation, thereby impairing their replication ability and achieving bacteriostasis[55]. In summary, these findings demonstrated that POGK hydrogel exhibited excellent antibacterial activity, effectively preventing pathogenic bacteria from infecting the wound.

The cytotoxicity of the hydrogels was investigated utilizing a CCK8 assay with HUVECs and NIH 3T3 cells. As depicted in Fig. 5c, the cell viability of both cell lines was unaffected when incubated with POG or POGK hydrogels, indicating the excellent cytocompatibility of both hydrogels. This desirable cytocompatibility is derived from the integral biocompatibility of all-natural products used in the hydrogels. Additionally, hemolysis evaluation was conducted to assess the blood compatibility of the hydrogels. Remarkably, the hemolysis rates of the hydrogels were found to be less than 2%, well below the permissible limit of 5% (Fig. 5d). Furthermore, the RBCs supernatants treated with the hydrogels were transparent and colorless compared to the positive control (Fig. 5d insert), demonstrating their good compatibility.

## Diabetic wound healing properties of hydrogels

According to the obtained results, the designed hydrogels possess the desired attributes of good adhesion, injectability, excellent antibacterial ability, and good biocompatibility. These characteristics underscore their potential as effective candidates for wound dressing applications. To evaluate their clinical therapeutic effects, a diabetic cutaneous wound model was established in diabetic mice (Fig. 6a). Based on a well-established method[56], the diabetic mice (with blood glucose values higher than 16.7 mmol·L$^{-1}$) were effectively established through the injection of streptozotocin into C57BL/6J mice (Supplementary Fig. S6). Mice diabetic wounds with an 8 mm diameter were induced and then treated with different materials, including sterile PBS (control), chitosan medical hydrogel (positive control), POG hydrogel, and POGK hydrogel. Macroscopic pictures of the injury healing process in various groups are shown in Fig. 6b. The remaining wound area in all groups progressively lowered gradually. In particular, the POGK hydrogel showed a superior area closure compared to the other groups (Fig. 6c), which could be attributed to the capacity to inhibit bacterial infection, reduce the inflammatory stage, and promote wound healing[45].

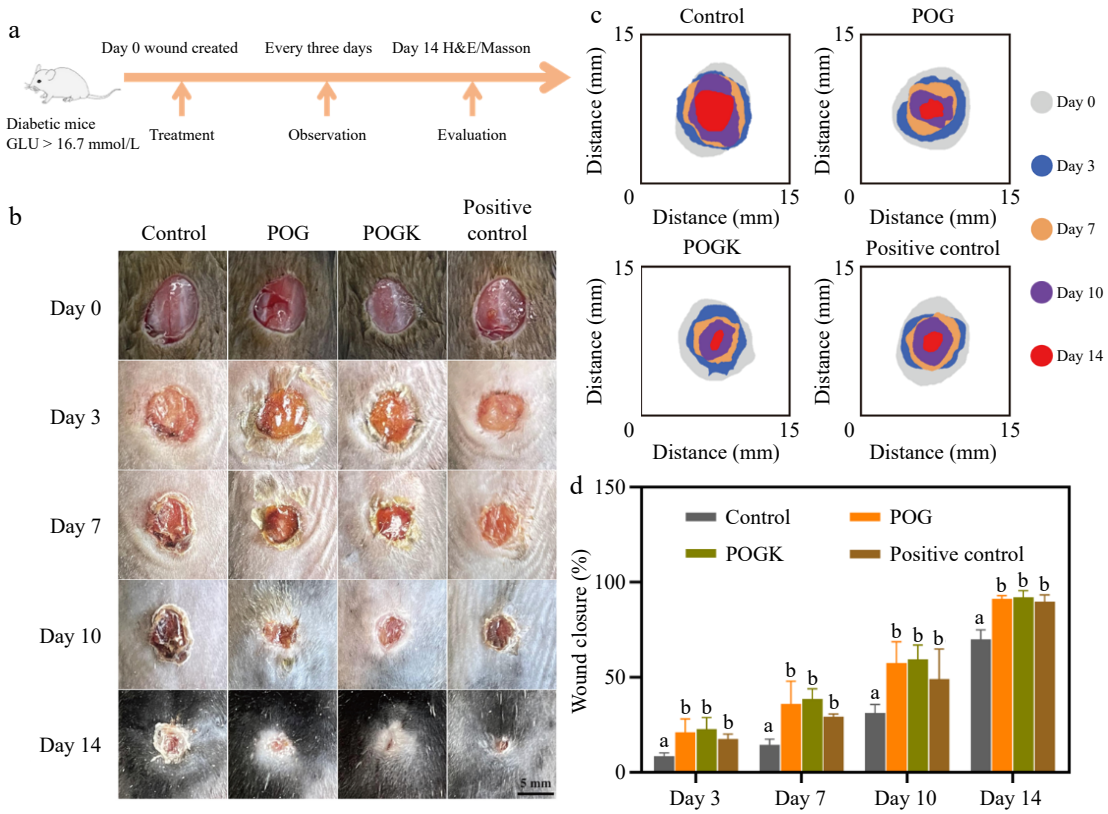


**Fig. 6** Treatment efficiency of the diabetic wound by the hydrogels in diabetic C57BL/6N mouse model. (a) Schematic illustration of a diabetic wound establishment and therapy schedule. (b) Depictive pictures of the diabetic wound recovery process. Scale bar: 5 mm. (c) Schematic representation of the wound healing throughout 14 d. (d) Quantification of the wound closure rate. Different letters in the histograms represent significant differences, $p < 0.05$.

The hydrogel-treated groups exhibited a markedly higher wound closure rate compared to the control group throughout the treatment period, with the POGK group showing a 59.5% wound contraction rate after 10 d compared to 31.2% in the control group (Fig. 6d). By day 14, the wounds in the POGK group were virtually completely closed, with a closure rate of 92.1%, while the control group displayed a significant unhealed area. The wound closure rate of the hydrogel treatment groups resembled that of the positive control group, indicating the prepared gels' efficacy in promoting wound healing. Although there were no significant differences in the wound repair capabilities of POG and POGK, it is important to note that the POGK gel with excellent antibacterial ability may accelerate the healing of bacterially infected wounds. Many studies have simulated bacterial infection in diabetic wounds by adding pathogenic bacteria and the results have actually shown that the antibacterial properties of hydrogel are crucial for injury recovery[57–59]. The results of this study support the idea that the POGK hydrogel's excellent antibacterial ability may contribute to accelerated healing in such cases. Overall, this study underscores the possibility of POGK hydrogels for diabetic injury recovery due to their combined antibacterial and stimuli-responsive activity.

## Histological analysis and angiogenesis *in vivo*

To further investigate the quality of the regenerated skin in the different treatment groups, histological analyses were conducted. As depicted in Fig. 7a, the results of H&E staining revealed a continuous and tightly coherent new epidermis in the hydrogel groups on day 14. In contrast, the injuries in the control group were not totally shut and the epidermal thickness was 28.62 ± 2.34 μm, significantly thinner than the epidermis of the hydrogel treatment groups (Fig. 7b). These H&E staining results aligned with the wound healing phenotype, indicating that the hydrogel groups exhibited superior healing efficiency, as evidenced by effective wound epithelialization.

Collagen deposition is essential for restoring the tensile strength of skin, promoting cell migration, and improving the healing process[60]. Therefore, Masson's staining was performed to assess collagen deposition on the injured tissue. The results revealed that all hydrogel groups displayed substantially greater collagen deposition compared to the control group after 14 d (Fig. 7a & c). Notably, the POGK hydrogel group exhibited tight and uniformly distributed collagen deposition at 51.6%, which is 1.65 times higher than the control group. Fibroblasts cross-linked with collagen have an effect on wound contraction throughout the healing process. Hyperglycemia has been reported to impair the healing process after injury by decreasing cell proliferation and affecting the synthesis of collagen[61]. Consequently, the reduced blood sugar levels achieved through enzyme catalysis may be responsible for the increased collagen deposition observed in the hydrogel groups. These histological results demonstrated that the POGK hydrogel could accelerate the healing of diabetic wounds by promoting re-epithelialization and enhancing collagen deposition.

New blood vessel formation is a critical indication of wound recovery, which impacts the delivery of different materials important for injury repair, such as oxygen, nutrients, and functional protein factors[62]. To evaluate whether the hydrogels could promote angiogenesis, Western blot experiments were performed to detect $\alpha$-smooth muscle actin ($\alpha$-SMA) and transforming growth factor $\beta$1 (TGF-$\beta$1), which play vital roles in neovascularization development and extracellular matrix protein accumulation[63,64]. As depicted in Fig. 8a–c and

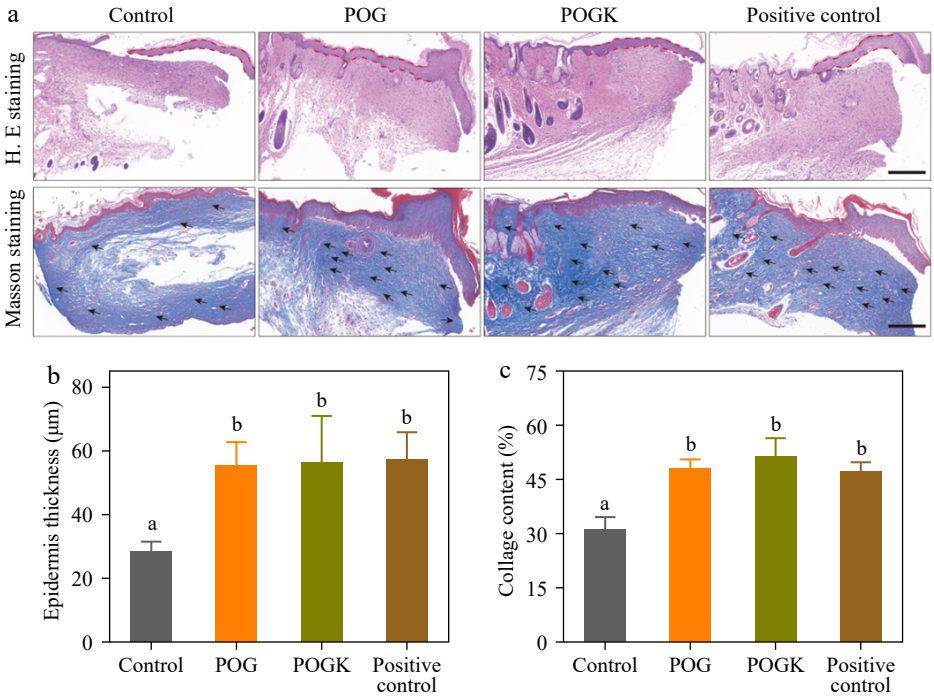


**Fig. 7** Histological analysis of wounds in different groups. (a) H&E and Masson's staining of injury tissues with different therapies on day 14. Scale bars = 200 μm. Metrological evaluation of (b) epidermis thickness, and (c) collagen deposition in each group on day 14. Different letters in the histograms indicate significant differences, $p < 0.05$.

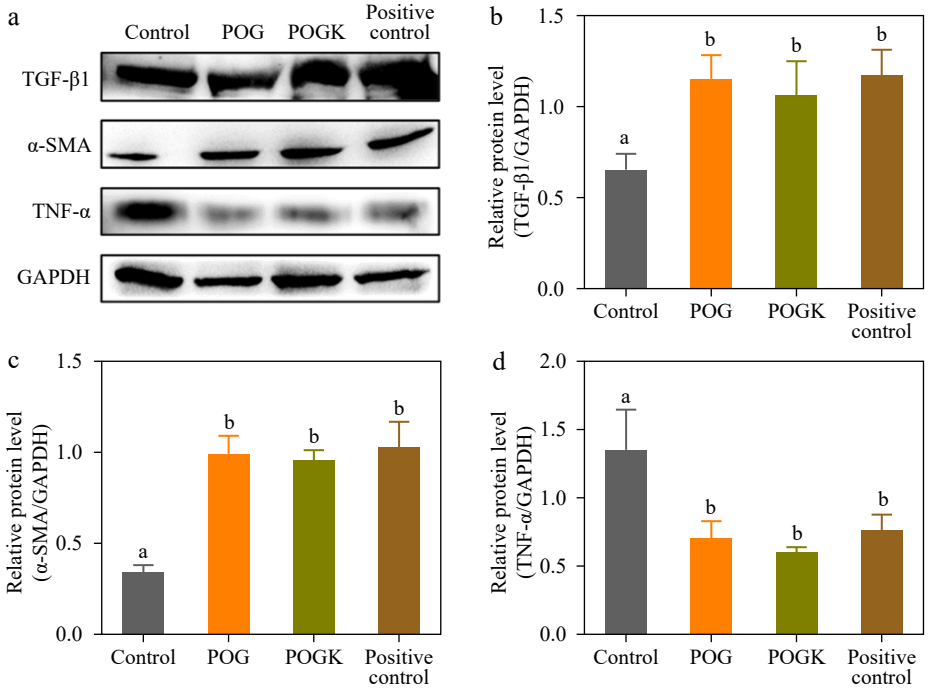


**Fig. 8** Result of hydrogels on protein expression in injury tissue. (a) Protein expression level of TGF-$\beta$1, $\alpha$-SMA, TNF-$\alpha$, and GAPDH detected by western blot in injury tissue with various therapies at day 14. Metrological evaluation of the relative protein expression level of (b) TGF-$\beta$1, (c) $\alpha$-SMA, and (d) TNF-$\alpha$. Different letters in the histograms indicate significant differences, $p < 0.05$.

Supplementary Fig. S7, the expression levels of $\alpha$-SMA and TGF-$\beta$1 in the wounds of the hydrogel-treated groups were significantly greater than those in the control group. The results suggested that the hydrogel groups formed more mature blood vessels, which could accelerate skin reconstruction by providing oxygen and nutrients. Additionally, tumor necrosis factor $\alpha$ (TNF-$\alpha$) was picked as an index to evaluate the inflammatory status of diabetic wounds. The hydrogel treatment groups displayed a reduced expression of TNF-$\alpha$ contrasted to the control group (Fig. 8a & d), indicating that the hydrogel possessed better anti-inflammatory effects, benefiting from its excellent antibacterial ability. In summary, these results revealed that the hydrogel can effectively alleviate inflammation and advertise angiogenesis and neovascularization, thereby accelerating diabetic wound healing.

## Conclusions

The administration of chronic wounds in patients with diabetes mellitus represents a significant clinical challenge, due to the increased susceptibility of these wounds to bacterial infection, persistent inflammation, and excessive reactive oxygen species. To address this issue, functional hydrogels were developed by cross-linking native, linear PM, and ODA polymers through the Schiff base reaction. The constructed hydrogels displayed an interconnected porous structure, excellent mechanical strength, and good tissue adhesion properties. Importantly, by encapsulating both amikacin and glucose oxidase during the hydrogel preparation, hydrogels with remarkable antibacterial activity and pH/glucose dual-responsiveness were produced, which is desirable for controlling drug release in the wound. Crucially, the animal studies demonstrated that these newly constructed hydrogels remarkably accelerated the healing of diabetic wounds by promoting re-epithelialization and collagen deposition. These findings indicate that the developed hydrogels have great promise for the repair of diabetic wounds and the regeneration of skin tissue.

## Author contributions

The authors confirm contribution to the paper as follows: study conception and design: Lv C, Zhao G, Zhang T; data collection: Yin S, Duan M, Wang Z; analysis and interpretation of results: Yin S, Zang J, Lv C, Zhang T, Fellner M; draft manuscript preparation: Yin S, Lv C, Zhang T; funding acquisition and supervision: Zhao G, Zhang T. All authors reviewed the results and approved the final version of the manuscript.

## Data availability

All data generated or analyzed during this study are included in this published article and its supplementary information files.

## Acknowledgments

This work was supported by National Key R & D Program of China (2021YFD2100100); the National Natural Science Foundation of China (31901638); and the 2115 Talent Development Program of China Agricultural University (109027). The authors thank Sun Mingyang and Qian Yiran for the animal experimental analysis.

## Conflict of interest

The authors declare that they have no conflict of interest.

**Supplementary information** accompanies this paper at (https://www.maxapress.com/article/doi/10.48130/fia-0024-0032)

## Dates

Received 27 July 2024; Revised 22 September 2024; Accepted 22 September 2024; Published online 22 October 2024

## References

1. Lim JZM, Ng NSL, Thomas C. 2017. Prevention and treatment of diabetic foot ulcers. *Journal of the Royal Society of Medicine* 110:104–9
2. Hauck S, Zager P, Halfter N, Wandel E, Torregrossa M, et al. 2021. Collagen/hyaluronan based hydrogels releasing sulfated hyaluronan improve dermal wound healing in diabetic mice via reducing inflammatory macrophage activity. *Bioactive Materials* 6:4342–59
3. Li Y, Fu R, Duan Z, Zhu C, Fan D. 2022. Artificial nonenzymatic antioxidant Mxene nanosheet-anchored injectable hydrogel as a mild photothermal-controlled oxygen release platform for diabetic wound healing. *ACS Nano* 16:7486–502
4. Wang T, Li Y, Cornel EJ, Li C, Du J. 2021. Combined antioxidant-antibiotic treatment for effectively healing infected diabetic wounds based on polymer vesicles. *ACS Nano* 15:9027–38
5. Chen H, Cheng Y, Tian J, Yang P, Zhang X, et al. 2020. Dissolved oxygen from microalgae-gel patch promotes chronic wound healing in diabetes. *Science Advances* 6:eaba4311
6. Tu C, Lu H, Zhou T, Zhang W, Deng L, et al. 2022. Promoting the healing of infected diabetic wound by an anti-bacterial and nano-enzyme-containing hydrogel with inflammation-suppressing, ROS-scavenging, oxygen and nitric oxide-generating properties. *Biomaterials* 286:121597
7. Mao C, Xiang Y, Liu X, Cui Z, Yang X, et al. 2018. Repeatable photodynamic therapy with triggered signaling pathways of fibroblast cell proliferation and differentiation to promote bacteria-accompanied wound healing. *ACS Nano* 12:1747–59
8. Zhang Z, Wang J, Luo Y, Li C, Sun Y, et al. 2023. A pH-responsive ZC-QPP hydrogel for synergistic antibacterial and antioxidant treatment to enhance wound healing. *Journal of Materials Chemistry B* 11:9300–10
9. Dong R, Guo B. 2021. Smart wound dressings for wound healing. *Nano Today* 41:101290
10. Xu Z, Han S, Gu Z, Wu J. 2020. Advances and Impact of Antioxidant Hydrogel in Chronic Wound Healing. *Advanced Healthcare Materials* 9:1901502
11. Gopinath D, Ahmed MR, Gomathi K, Chitra K, Sehgal PK, et al. 2004. Dermal wound healing processes with curcumin incorporated collagen films. *Biomaterials* 25:1911–17
12. Peng Y, He D, Ge X, Lu Y, Chai Y, et al. 2021. Construction of heparin-based hydrogel incorporated with Cu5.4O ultrasmall nanozymes for wound healing and inflammation inhibition. *Bioactive Materials* 6:3109–3124
13. Choi H, Kim B, Jeong SH, Kim TY, Kim DP, et al. 2023. Microalgae-based biohybrid microrobot for accelerated diabetic wound healing. *Small* 19:2204617
14. Yuan Y, Fan D, Shen S, Ma X. 2022. An M2 macrophage-polarized anti-inflammatory hydrogel combined with mild heat stimulation for regulating chronic inflammation and impaired angiogenesis of diabetic wounds. *Chemical Engineering Journal* 433:133859
15. Alfei S, Schito GC, Schito AM, Zuccari G. 2024. Reactive oxygen species (ROS)-mediated antibacterial oxidative therapies: available methods to generate ROS and a novel option proposal. *International Journal of Molecular Sciences* 25:7182
16. Lu Y, Li H, Wang J, Yao M, Peng Y, et al. 2021. Engineering bacteria-activated multifunctionalized hydrogel for promoting diabetic wound healing. *Advanced Functional Materials* 31:2105749
17. Shi T, Lu H, Zhu J, Zhou X, He C, et al. 2023. Naturally derived dual dynamic crosslinked multifunctional hydrogel for diabetic wound healing. *Composites Part B - Engineering* 257:110687
18. Hu B, Gao M, Boakye-Yiadom KO, Ho W, Yu W, et al. 2021. An intrinsically bioactive hydrogel with on-demand drug release behaviors for diabetic wound healing. *Bioactive Materials* 6:4592–606
19. Liang Y, He J, Guo B. 2021. Functional hydrogels as wound dressing to enhance wound healing. *ACS Nano* 15:12687–722
20. Hu C, Zhang F, Long L, Kong Q, Luo R, et al. 2020. Dual-responsive injectable hydrogels encapsulating drug-loaded micelles for on-demand antimicrobial activity and accelerated wound healing. *Journal of Controlled Release* 324:204–17
21. Hu J, Hu Q, He X, Liu C, Kong Y, et al. 2020. Stimuli-responsive hydrogels with antibacterial activity assembled from guanosine, aminoglycoside, and a bifunctional anchor. *Advanced Healthcare Materials* 9:1901329
22. Nonsuwan P, Matsugami A, Hayashi F, Hyon SH, Matsumura K. 2019. Controlling the degradation of an oxidized dextran-based hydrogel independent of the mechanical properties. *Carbohydrate Polymers* 204:131–41
23. Guan S, Zhang K, Cui L, Liang J, Li J, et al. 2022. Injectable gelatin/oxidized dextran hydrogel loaded with apocynin for skin tissue regeneration. *Biomaterials Advances* 133:112604
24. Wu Y, Wang Y, Long L, Hu C, Kong Q, et al. 2022. A spatiotemporal release platform based on pH/ROS stimuli-responsive hydrogel in wound repairing. *Journal of Controlled Release* 341:147–65
25. Albright V, Zhuk I, Wang YH, Selin V, van de Belt-Gritter B, et al. 2017. Self-defensive antibiotic-loaded layer-by-layer coatings: Imaging of localized bacterial acidification and pH-triggering of antibiotic release. *Acta Biomaterialia* 61:66–74
26. Fang X, Liu Y, Zhang M, Zhou S, Cui P, et al. 2022. Glucose oxidase loaded thermosensitive hydrogel as an antibacterial wound dressing. *Journal of Drug Delivery Science and Technology* 76:103791
27. Wang L, Chen G, Fan L, Chen H, Zhao Y, et al. 2023. Biomimetic enzyme cascade structural color hydrogel microparticles for diabetic wound healing management. *Advanced Science* 10:2206900
28. Qi W, Yan X, Fei J, Wang A, Cui Y, et al. 2009. Triggered release of insulin from glucose-sensitive enzyme multilayer shells. *Biomaterials* 30:2799–806
29. Wang Y, Wang J, Gao R, Liu X, Feng Z, et al. 2022. Biomimetic glycopeptide hydrogel coated PCL/nHA scaffold for enhanced cranial bone regeneration via macrophage M2 polarization-induced osteo-immunomodulation. *Biomaterials* 285:121538
30. Khoury LR, Slawinski M, Collison DR, Popa I. 2020. Cation-induced shape programming and morphing in protein-based hydrogels. *Science Advances* 6:eaba6112
31. Zhang Q, Liu Y, Yang G, Kong H, Guo L, et al. 2023. Recent advances in protein hydrogels: From design, structural and functional regulations to healthcare applications. *Chemical Engineering Journal* 451:138494
32. Jia Y, Li J. 2015. Molecular assembly of Schiff Base interactions: construction and application. *Chemical Reviews* 115:1597–621
33. Liu W, Liu S, Sun M, Guo F, Wang P, et al. 2024. Glycopeptide-based multifunctional nanofibrous hydrogel that facilitates the healing of diabetic wounds infected with methicillin-resistant Staphylococcus aureus. *Acta Biomaterialia* 181:161–75
34. Zhou X, Zhao B, Wang L, Yang L, Chen H, et al. 2023. A glucose-responsive nitric oxide release hydrogel for infected diabetic wounds treatment. *Journal of Controlled Release* 359:147–60
35. Hou F, Jiang W, Zhang Y, Tang J, Li D, et al. 2022. Biodegradable dual-crosslinked adhesive glue for fixation and promotion of osteogenesis. *Chemical Engineering Journal* 427:132000
36. Yin SH, Duan MP, Qian YR, Lv CY, Zang JC, et al. 2023. Regulatable and reversible native paramyosin hydrogels promote the wound healing of the skin in mice. *Chemical Engineering Journal* 462:142294

37. Zhang M, Chen G, Lei M, Lei J, Li D, et al. 2021. A pH-sensitive oxidized-dextran based double drug-loaded hydrogel with high antibacterial properties. *International Journal of Biological Macromolecules* 182:385−93
38. Yan S, Wang T, Feng L, Zhu J, Zhang K, et al. 2014. Injectable in situ self-cross-linking hydrogels based on poly(L-glutamic acid) and alginate for cartilage tissue engineering. *Biomacromolecules* 15:4495−508
39. Huang Y, Mu L, Zhao X, Han Y, Guo B. 2022. Bacterial growth-induced tobramycin smart release self-healing hydrogel for *Pseudomonas aeruginosa*-infected burn wound healing. *ACS Nano* 16:13022−36
40. Tan W, Long T, Wan Y, Li B, Xu Z, et al. 2023. Dual-drug loaded polysaccharide-based self-healing hydrogels with multifunctionality for promoting diabetic wound healing. *Carbohydrate Polymers* 312:120824
41. Lü SY, Gao CM, Xu XB, Bai X, Duan HG, et al. 2015. Injectable and Self-Healing Carbohydrate-Based Hydrogel for Cell Encapsulation. *Acs Applied Materials & Interfaces* 7:13029−37
42. Xue X, Hu Y, Deng Y, Su J. 2021. Recent advances in design of functional biocompatible hydrogels for bone tissue engineering. *Advanced Functional Materials* 31:2009432
43. Zhao Y, Li Z, Song S, Yang K, Liu H, et al. 2019. Skin-inspired antibacterial conductive hydrogels for epidermal sensors and diabetic foot wound dressings. *Advanced Functional Materials* 29:1901474
44. Bertsch P, Diba M, Mooney DJ, Leeuwenburgh SCG. 2023. Self-healing injectable hydrogels for tissue regeneration. *Chemical Reviews* 123:834−873
45. Fu YJ, Shi YF, Wang LY, Zhao YF, Wang RK, et al. 2023. All-Natural Immunomodulatory Bioadhesive Hydrogel Promotes Angiogenesis and Diabetic Wound Healing by Regulating Macrophage Heterogeneity. *Advanced Science* 10:2206771
46. Han X, Chen S, Cai Z, Zhu Y, Yi W, et al. 2023. A Diagnostic and Therapeutic Hydrogel to Promote Vascularization via Blood Sugar Reduction for Wound Healing. *Advanced Functional Materials* 33:2213008
47. Zhao L, Niu L, Liang H, Tan H, Liu C, et al. 2017. pH and glucose dual-responsive injectable hydrogels with insulin and fibroblasts as bioactive dressings for diabetic wound healing. *ACS Applied Materials & Interfaces* 9:37563−74
48. Wallace LA, Gwynne L, Jenkins T. 2019. Challenges and opportunities of pH in chronic wounds. *Therapeutic Delivery* 10:719−35
49. Shao Z, Yin T, Jiang J, He Y, Xiang T, et al. 2023. Wound microenvironment self-adaptive hydrogel with efficient angiogenesis for promoting diabetic wound healing. *Bioactive Materials* 20:561−73
50. Hao J, Liu CX, Zhou L, Wu N, Sun MY, et al. 2024. Enhancing diabetic wound healing with a pH/glucose dual-responsive hydrogel for ROS clearance and antibacterial activity. *International Journal of Biological Macromolecules* 272:132935
51. Zhu S, Zhao B, Li M, Wang H, Zhu J, et al. 2023. Microenvironment responsive nanocomposite hydrogel with NIR photothermal therapy, vascularization and anti-inflammation for diabetic infected wound healing. *Bioactive Materials* 26:306−320
52. Yang Y, Zhao X, Yu J, Chen X, Wang R, et al. 2021. Bioactive skin-mimicking hydrogel band-aids for diabetic wound healing and infectious skin incision treatment. *Bioactive Materials* 6:3962−75
53. Maleki A, He J, Bochani S, Nosrati V, Shahbazi MA, et al. 2021. Multifunctional photoactive hydrogels for wound healing acceleration. *ACS Nano* 15:18895−930
54. Thorn CR, Carvalho-Wodarz CdS, Horstmann JC, Lehr CM, Prestidge CA, Thomas N. 2021. Tobramycin liquid crystal nanoparticles eradicate cystic fibrosis-related *pseudomonas aeruginosa* biofilms. *Small* 17:2100531
55. Zi Y, Zhu M, Li X, Xu Y, Wei H, et al. 2018. Effects of carboxyl and aldehyde groups on the antibacterial activity of oxidized amylose. *Carbohydrate Polymers* 192:118−25
56. Furman BL. 2021. Streptozotocin-induced diabetic models in mice and rats. *Current Protocols* 1:e78
57. Deng M, Wu Y, Ren Y, Song H, Zheng L, et al. 2022. Clickable and smart drug delivery vehicles accelerate the healing of infected diabetic wounds. *Journal of Controlled Release* 350:613−29
58. Hu C, Long L, Cao J, Zhang S, Wang Y. 2021. Dual-crosslinked mussel-inspired smart hydrogels with enhanced antibacterial and angiogenic properties for chronic infected diabetic wound treatment via pH-responsive quick cargo release. *Chemical Engineering Journal* 411:128564
59. Li Y, Su L, Zhang Y, Liu Y, Huang F, et al. 2022. A guanosine-quadruplex hydrogel as cascade reaction container consuming endogenous glucose for infected wound treatment-a study in diabetic mice. *Advanced Science* 9:2103485
60. Wang Z, Dong Y, Wang Y. 2023. Collagen-based biomaterials for tissue engineering. *ACS Biomaterials Science & Engineering* 9:1132−50
61. Azevedo F, Pessoa A, Moreira G, Dos Santos M, Liberti E, et al. 2016. Effect of topical insulin on second-degree burns in diabetic rats. *Biological Research for Nursing* 18:181−92
62. Eming SA, Brachvogel B, Odorisio T, Koch M. 2007. Regulation of angiogenesis: wound healing as a model. *Progress in Histochemistry and Cytochemistry* 42:115−70
63. Liang Y, Li M, Yang Y, Qiao L, Xu H, et al. 2022. pH/Glucose dual responsive metformin release hydrogel dressings with adhesion and self-healing via dual-dynamic bonding for athletic diabetic foot wound healing. *ACS Nano* 16:3194−207
64. Wynn TA, Vannella KM. 2016. Macrophages in tissue repair, regeneration, and fibrosis. *Immunity* 44:450−62